Simulation of the response of an ionization chamber to ^{214}Bi emission. Application to the measurement of ^{222}Rn.

Sylvie Pierre, Cheick Thiam, Philippe Cassette, Xavier Mougeot, Abhilasha Singh

Simulation of the response of an ionization chamber to ^{214}Bi emission. Application to the measurement of ^{222}Rn.

Sylvie Pierre*, Cheick Thiam, Philippe Cassette, Xavier Mougeot, Abhilasha Singh.

CEA, LIST, Laboratoire National Henri Becquerel (LNE-LNHB), Bât 602, PC111, CEA-Saclay, 91191 Gif-sur-Yvette, Cedex, France

*Corresponding author. Sylvie Pierre; Tel.: +33 1 69 08 43 75; Fax: +33 1 69 08 26 19.

E-mail address: sylvie.pierre@cea.fr

Abstract

PENELOPE simulations of a Vinten ionization chamber (IC) were performed to investigate the influence of the thickness of glass-ampoules used in ^{222}Rn standardization. The simulation reveals a non-negligible variation of the energy deposited in the chamber gas region (which may induce a proportional variation of the measured current) when considering the β transition emissions of the daughters of ^{222}Rn. This reinforces the idea of using a specialist container (made of metal to preserve the integrity of the container) that would circulate between the metrology laboratories in the context of international comparison exercises using the BIPM international reference system (SIR)..

Keywords: Ionization chamber, Monte Carlo simulation, PENELOPE, Radionuclide metrology, Radon.

1. Introduction

Well-type ionization chambers (ICs), connected to current-measuring electronics, are activity measurement instruments commonly used in nuclear medicine services, national metrology institutes (NMI) or radiopharmaceutical industry. It is also the transfer instrument used for the Système International de Référence (SIR) for activity comparison at the Bureau International des Poids et Mesures (BIPM) (Rytz, 1983, Ratel, 2007). The accuracy of the results and the ease of measurement explain the choice of this technique. The response of such instruments *i.e.,* the measured ionization current (which is related to the total energy deposited in the IC gas volume), depends on the chamber design (wall thickness, nature and pressure of the filling gas), the nature and dimensions of the source (type of vial or ampoule, filling height of radioactive sample, etc.), and the shielding around (Ceccatelli et al., 2007; Kryeziu et al., 2007; Thiam et al., 2016). Generally, ICs are well adapted for solutions of gamma-emitting radionuclides (Amiot et al., 2012; Zimmerman and Judge, 2007) but can also be used for high-energy beta-emitting radionuclides such as ^{90}Y, although such measurements are more challenging (Pearce et al, 2007; Fenwick et al., 2014). In these cases, the IC response strongly depends on the transport of electrons in the radioactive solution and surroundings.

A few years ago, measurements of gaseous ^{222}Rn samples contained in sealed glass ampoules, were performed with ICs at different NMIs and at the BIPM, in the context of a comparison using the SIR (BIPM.RI(II)-K1.Rn222). This comparison has highlighted relative differences of almost 5 % between laboratories and the results were not consistent within their uncertainties (Michotte et al., 2012). This issue has not yet been solved and gas glass ampoules are still being used to compare radon standards for submissions to the SIR.

More recently, bias in measurements of gaseous ^{222}Rn using ICs were investigated at the LNHB (Pierre et al., 2018). In this previous work, several measurements were carried out at the LNHB and at the BIPM and the variability of the response of ICs was investigated by considering the volume of the ampoule, the position of the sealing point and the thickness of the ampoule's base, which does not play a major role. The conclusion of this study highlighted that the variability of these gas glass ampoules could induce a measurement bias higher than the uncertainty of standard sources. Discrepancies observed were then interpreted to be the consequence of the contribution of high-energy electrons released from the main β-emitting daughters of ^{222}Rn, in particular ^{214}Bi (maximum beta energy of 3.27 MeV). These electrons have enough energy to reach directly the counting gas of the chamber (Michotte at al., 2006).

In order to address this phenomenon, we present here an additional study based on the Monte Carlo simulation of the Vinten type 671 IC (the IC used at the LNHB for standard transfers) with ^{222}Rn gas glass ampoules. It has to be noted that the ionization of the IC gas is mainly due to the gamma emissions above a certain energy threshold (about 25 keV for the Vinten Chamber). However, high-energy electrons released by the ^{222}Rn daughters such as ^{241}Bi or ^{210}Tl may contribute to the IC response via the Bremsstrahlung photons created in the solution itself, the container (the ampoule in this case), the holder walls and the inner wall of the chamber. In addition, electrons with the highest energies can reach directly the IC gas volume and interact with a high probability.

2. Methods

2.1 Decay scheme of radon

^{222}Rn is a radioactive noble gas decaying through alpha transition (Fig. 1) to short half-life solid progenies and is one of the main sources of natural radioactivity.

National standards of ^{222}Rn are available in several countries and comparison of these standards is necessary to ensure the international traceability of ^{222}Rn measurement and to support the Calibration and Measurement Capabilities (CMCs) of the National Metrology Institutes.

The equilibrium with short-lived progenies (except for ^{210}Pb and daughters) is obtained after 4 hours. Table 1 shows the ratio between ^{222}Rn and its daughters after 4 hours, having reached equilibrium.

2.2. Description of the simulations

The dependence of ^{222}Rn results on ampoule geometry was studied by means of MC simulations of the LNHB Vinten chamber, based on original work by De Vismes and Amiot (2003) and Amiot (2004). The Vinten IC, designed on the basis of the IG42 IC constructed by Centronic (Woods et al., 1983), is used in routine at LNHB as a transfer instrument. The IC is composed of a cylindrical aluminium chamber (with a 10.5 L effective volume filled with N_2 at 1 MPa) with a coaxial re-entrant well, made of aluminium. The IC ionization current is collected via a central aluminium alloy electrode. The chamber is housed in a locally made shielding in order to reduce the background. The PENELOPE simulation model of this chamber (geometry and sample-to-detector configuration) has been well-validated through different comparisons and for several gamma-emitting radionuclides (Amiot et al., 2012). The geometry used in our work is shown in Fig. 2.

Simulations were performed using PENELOPE code (version 2014) (Salvat, 2015; Baró, 1995) and Geant4 code (version geant4.10.0) (Agostinelli et al., 2003), studying the influence of the ampoule wall-thickness and the type (glass or metal), focusing on the ^{214}Bi daughter nuclide.

For a given radionuclide, the calibration coefficient (C_f in A/MBq) can be deduced from the total energy deposited in the gas E_d (eV) (obtained with PENELOPE calculations) according to the expression: $C_f = e \times E_d / W$, where e is the electron charge and W the mean energy needed to produce an ion pair in the IC counting gas. Therefore, the variability observed in E_d reflects the variability of the calibration coefficient.

Usually, the calibration is carried out with glass gas ampoules with a wall thickness of approximately 1.3 mm, filled with ^{222}Rn gas at very low pressure. It should be noted that for the SIR comparison BIPM.RI(II)-K1.Rn-222 (Michotte et al 2012), the ampoules submitted to the BIPM were all filled with a very low pressure. No specification was requested from the ampoule's supplier. As it was noticed that the thickness could be thicker than the nominal value, the simulations were performed at different thicknesses from 1.0 mm to 1.9 mm in steps of 0.1 mm.

2.3 ^{222}Rn simulation

As it is very difficult and very time consuming to simulate the total disintegration chain of ^{222}Rn, and also because the IC instruments are not sensitive to alpha-emissions, the simulations were focussed on the daughters ^{214}Bi and ^{210}Tl radionuclides, which are assumed to influence IC response due to their high-energy β-emissions (Table 1).

The emitted particles by the selected daughter radionuclides are randomly generated as a uniform distribution in the whole volume of the radon source. In practice, when filling the radon ampoule, the solid daughters are on the ampoule walls, but considering the negligible pressure in the ampoules, using the volume source has no impact on the results. The initial electron energies emitted in the case of the beta transitions were taken from spectra calculated with the BetaShape program (Mougeot, 2016). Simulations were performed with a large number of primary events (about 10^8 histories) in order to obtain good statistical precision of the result (i.e., the total energy deposited in the counting gas region deduced by averaging over all histories), below 1 %.

3. Results and discussion

Fig. 3 presents the average total energy deposition in the IC gas region (corrected by the ratios reported in Table 1) when we simulate only the β−transition emissions of ^{222}Rn daughters, for glass ampoules with a nominal wall thickness of 1.3 mm. For Bi, Tl, Pb we used the total beta spectrum resulting from all the transitions. In this respect and considering the ratios given in Table 1, we can consider that ^{214}Bi represents the main daughter able to introduce a non-negligible contribution of direct ionization of the counting gas through its β-emissions.

Simulations were then focused on ^{214}Bi by considering individually the branches $\beta^-_{0,0}$ (3.27 MeV with a probability of ~19.6 %) and $\beta^-_{0,11}$ (1.5 MeV with a probability of ~17.5 %), and, finally, the total spectrum of all transitions.

The plot in Fig. 4 displays the variation of the total mean energy deposited in the IC gas region per decay as a function of ampoule thickness with the ^{214}Bi total beta spectrum. Only statistical uncertainties of the MC simulations are considered here in the plot (~ 0.3 %). A decrease of the energy deposition in the chamber sensitive volume according to the ampoule thickness is clearly observed. This correlation yields a constant difference of about 14 % when we increase the thickness in steps of 0.1 mm.

To verify these results, the simulations were reproduced with another high-energy β-emitting daughter in the ^{222}Rn decay chain, ^{210}Tl. The individual branches $\beta^{-}_{0,3}$ (~ 4.3 MeV with a probability of ~31 %) and $\beta^{-}_{0,2}$ (~ 4.4 MeV with a probability of ~13 %) as well as the total spectrum were considered. For the total spectrum, the observed behaviour (Fig. 4) is comparable to that of ^{214}Bi. The simulations for ^{214}Bi as well as ^{210}Tl (total β spectra) also show that the contribution of β transitions can be reduced to nearly zero when a 1 mm thick copper attenuator is positioned around the ampoules (Fig. 4 and 6).

For the individual branches $\beta^{-}_{0,3}$ and $\beta^{-}_{0,2}$ of ^{210}Tl, the same behaviour as for the total spectrum can be observed (Fig. 5). A similar behaviour was observed for the individual transitions of ^{214}Bi (not shown).

To investigate the influence of the nature of ampoules, we have also performed similar simulations using aluminium ampoules instead of glass, with the same variation of thickness. This resulted in a comparable behaviour of aluminium albeit at higher attenuation as one can see in Fig. 6 for the total β spectrum of ^{214}Bi. Again, a comparable behaviour of an aluminium versus a glass ampoule was observed for ^{210}Tl (not shown).

In view of these results, we can highlight that the contribution of the high-energy electrons released from ^{214}Bi decays significantly depends on the ampoule wall-thickness: a 0.1 mm variation in the wall thickness variation results in a 14% relative variation of the total energy deposited in the IC gas volume by the electrons. Even if this variation must be put in perspective with the response of IC to all the gamma emissions of the ^{222}Rn daughter nuclides not considered in the present study, this sensitivity may well be at the origin of discrepancies observed in the SIR.

4. Conclusions

In the context of the SIR, ICs are used to compare ^{222}Rn standards. In the past, when using gas-filled glass ampoules, discrepancies between measurements remained unexplained (BIPM.RI(II)-K1.Rn222). In this work, the problem of the uncertainty of IC response due to the variability of the original glass ampoules used for ^{222}Rn measurements was investigated by means of MC calculations. The objective was to check if the ampoule thickness could influence the response of the IC, by considering the high-energy electrons of the β transitions from the ^{222}Rn decay chain radionuclides. It must be highlighted that Pearce et al. (2007) mentioned that "the simulation of IC response curves to beta emission is very sensitive to internal geometry of the IC and of the source, especially when the electron energy is high enough to cross all the layers and reach the gaseous sensitive volume". The results of the MC simulations of some ^{222}Rn daughter radionuclides highlight a systematic and non-negligible correlation between the IC gas ionization and the variation of the wall thickness of the ampoules used in measurements. As consequence of this work and previous studies, a possible solution to reduce the high discrepancies, observed for instance in the frame of the SIR comparison, would be to use a specialist container for ^{222}Rn that could be circulated between the participating laboratories. This ampoule can be made of Al with an optimised geometry (Bailat, 2016) in order to preserve the integrity of the sample during different displacements. As far as everyone would use the same ampoule, the properties of this ampoule do not need to be studied. If the glass gas ampoules are still to be used for comparisons, it could be useful to add to the protocol that a copper attenuator should be placed around the ampoule. It must be noted that the pressure effect of ^{222}Rn ampoules has not been investigated in this study but could also be a source of uncertainty. However, the submitted ampoules during the BIPM.RI(II)-K1.Rn222 comparison were approximately at the same low pressure, therefore the contribution of this should be significantly less than the 5% discrepancies observed.

Acknowledgments

The authors want to thank Marie-Noëlle Amiot for providing them with the geometry file of the IC, and Vanessa Chisté for her advice and comments.

References

Agostinelli, S., et al., 2003. Geant4 – a simulation toolkit. Nucl. Instrum. Meth. A 506, 250-303.

Amiot, M.-N., 2004. Calculation of ^{18}F, ^{99m}Tc, ^{111}In and ^{123}I calibration factor using the PENELOPE ionization chamber simulation method, Appl. Radiat. Isot. 60, 529-533.

Amiot, M.-N., Mesradi, M.R., Chisté, V., Morin, M., Rigoulay, F., 2012. Comparison of experimental and calculated calibration coefficients for a high sensitivity ionization chamber. Appl. Radiat. Isot. 70, 2232–2236.

Bailat, C., 2016, Pers. Commun.

Baró, J et al., 1995. PENELOPE: An algorithm for Monte Carlo simulation of the penetration and energy loss of electron and positrons in matter. Nucl. Instrum. Methods B 100, 31-46.

Ceccatelli, A., Benassi, M., D'Andrea, M., De Felice, P., Fazio, A., Nocentini, S., Strigari, L., 2007. Experimental determination of calibration settings of a commercially available radionuclide calibrator for various clinical measurement geometries and radionuclides. Appl. Radiat. Isot. 65, 120–125.

De Vismes, A., Amiot, M.-N., 2003. Towards absolute activity measurements by ionisation chambers using the PENELOPE Monte-Carlo code. Appl. Radiat. Isot. 59, 267-272.

Fenwick, A., Baker, M., Ferreira, K., Keightley, J., 2014. Comparison of ^{90}Y and ^{177}Lu measurement capability in UK and European hospitals. Appl. Radiat. Isot. 87, 10-13.

Kryeziu, D., Tschurlovits, D., Kreuziger, M., Maringer, F.-J., 2007. Calculation of calibration figures and the volume correction factors for ^{90}Y, ^{125}I, ^{131}I and ^{177}Lu radionuclides based on Monte-Carlo ionization chamber simulation method. Nucl. Instrum. Meth. A 580, 250–253.

Michotte, C., Pearce, A.K., Cox, M.G., Gostely, J.-J., 2006. An approach based on the SIR measurement model for determining the ionization chamber efficiency curves, and a study of ^{65}Zn and ^{201}Tl photon emission intensities. Appl. Radiat. Isot. 64, 1147-1155.

Michotte, C., Ratel, G., and Cassette, P. 2012. Update of the BIPM.RI(II)-K1.Rn-222 comparison of activity measurements for the radionuclide 222Rn to include the LNE–LNHB, France. Metrologia 49 Tech. Suppl. 06001.

Mougeot, X., 2016. Systematic comparison of beta spectra calculations using improved analytical screening correction with experimental shape factors. Appl. Radiat. Isot. 109, 177-182.

Pearce, A. K., Michotte, C., and Hino, Y., Ionization chamber efficiency curves. Metrologia **44** (2007) S67-S70.

Pierre, S., et al., 2018. Bias in the measurement of radon gas using ionization chambers: Application to SIR. Appl. Radiat. Isot. 134, 13-17.

Ratel, G., 2007. The Système International de Référence and its application in key comparisons, Metrologia, 44(4), S7-S16.

Rytz, A., 1983. The international reference system for activity measurements of γ-ray emitting nuclides. Appl. Radiat. Isot. 34 (8), 1047–1056.

Salvat, F., 2015. PENELOPE-2014: A Code System for Monte Carlo Simulation of Electron and Photon Transport, OECD NEA Data Bank, NEA/NSC/DOC(2015)3

Thiam, C., et al., 2016. Investigation of the response variability of ionization chambers for the standard transfer of SIR-Spheres. Appl. Radiat. Isot. 109, 231-235.

Woods, M.J., Callow, W.J., Christmas, P., 1983. The NPL radionuclides calibrator-Type 27. Int. J. Nucl. Med. Biol. 10, 127-132.

Zimmerman, B.E., Judge, S., 2007. Traceability in nuclear medicine. Metrologia 44, S127-S132.

Figure captions:

Fig. 1: Decay scheme of ^{222}Rn.

Fig. 2: View of the geometry of the chamber modelled. The hatching indicated by letter A corresponds to the radon source.

Fig. 3: Average of total energy deposition in IC gas region for β^- transition emissions of the ^{222}Rn daughters, plotted on a log scale. This plot takes into account the ratio reported in Table 1.

Fig. 4: Variation of the mean energy deposited in the IC counting gas region per decay as a function of the radon ampoule wall thickness (with and without 1 mm copper attenuator), for the total spectrum. This plot does not take into account the ratio reported in Table 1.

Fig. 5: Average of total energy deposition in the IC counting gas region per decay for the transitions $\beta^-_{0,2}$ and $\beta^-_{0,3}$ of ^{210}Tl. This plot does not take into account the ratio reported in Table 1.

Fig. 6: Variation of the mean energy deposited in the IC counting gas region per decay as a function of the radon ampoule wall thickness (in glass or aluminium) for ^{214}Bi and ^{210}Tl (with and without 1 mm copper attenuator), for the total spectrum. Simulations made with Geant4. This plot does not take into account the ratio reported in Table 1.

Table captions:

Table 1: Activity ratio between ^{222}Rn and progenies after 4 hours and major modes of decay.

Fig. 1.

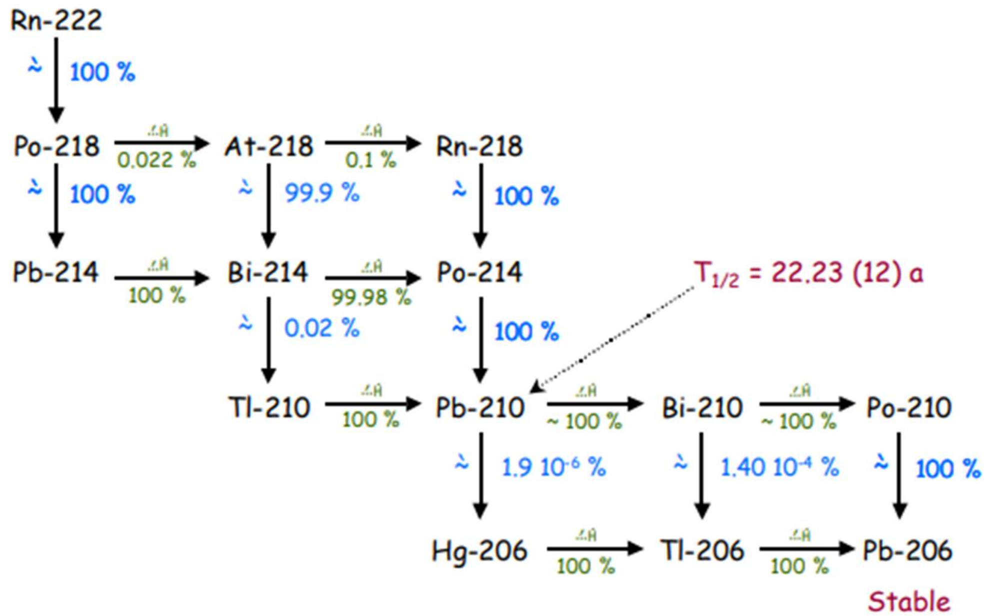
Rn-222
100 %
Po-218
0,022 %
At-218
0,1 %
Rn-218
100 %
99,9 %
100 %
Pb-214
100 %
Bi-214
99,98 %
Po-214
$T_{1/2}$ = 22,23 (12) a
0,02 %
100 %
Tl-210
100 %
Pb-210
~ 100 %
Bi-210
~ 100 %
Po-210
1,9 10-6 %
1,40 10-4 %
100 %
Hg-206
100 %
Tl-206
100 %
Pb-206
Stable

Fig. 2.

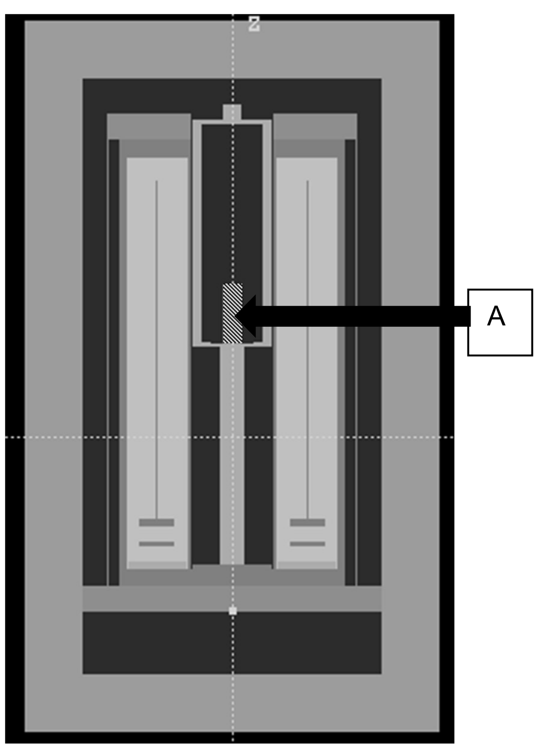
A

Fig. 3.

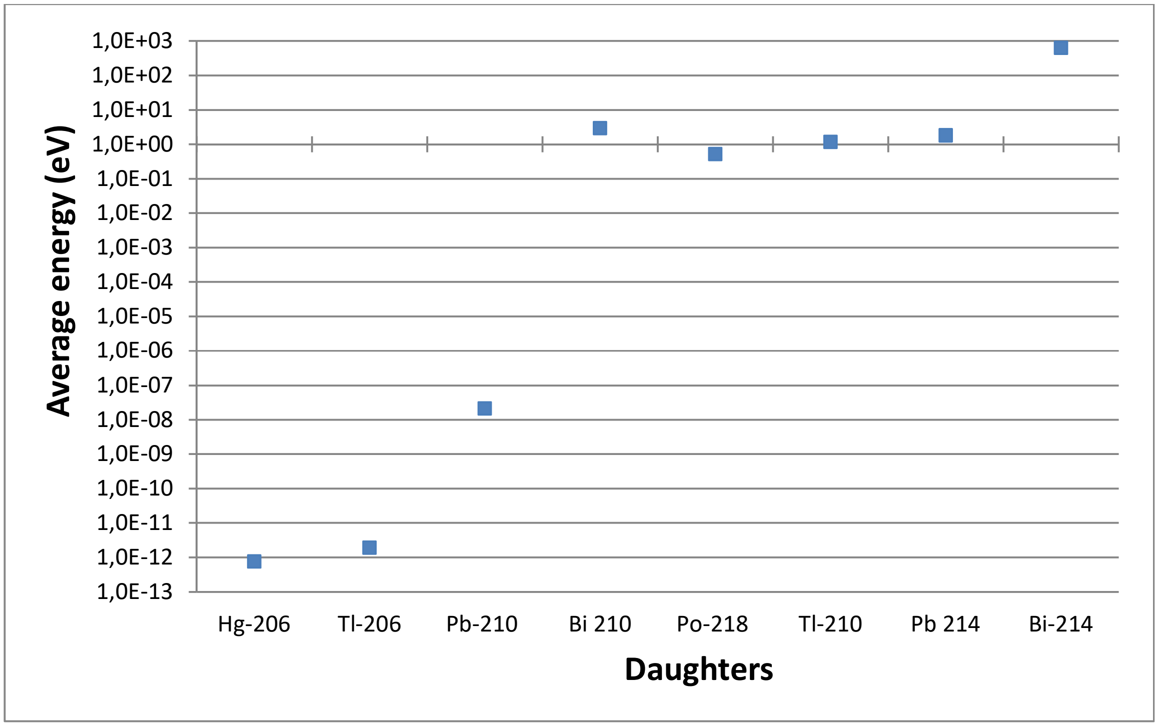
1,0E+03
1,0E+02
1,0E+01
1,0E+00
1,0E-01
1,0E-02
1,0E-03
1,0E-04
1,0E-05
1,0E-06
1,0E-07
1,0E-08
1,0E-09
1,0E-10
1,0E-11
1,0E-12
1,0E-13
Average energy (eV)
Hg-206
Tl-206
Pb-210
Bi 210
Po-218
Tl-210
Pb 214
Bi-214
Daughters

Fig. 4.

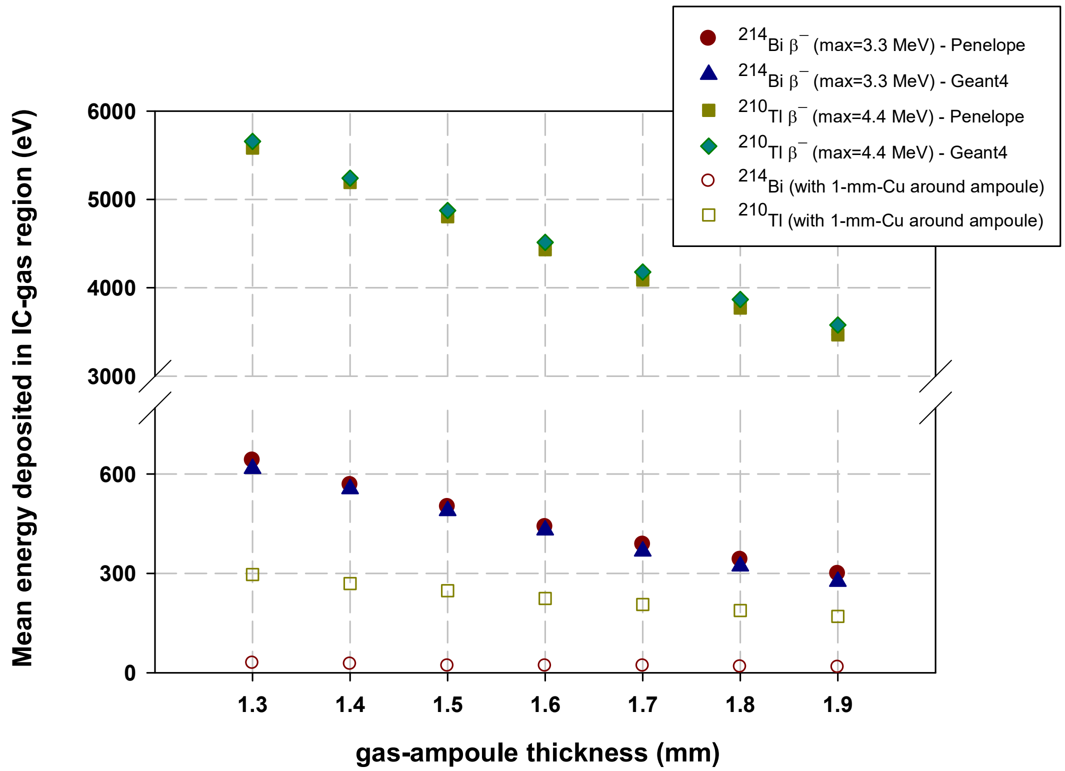
214Bi β⁻ (max=3.3 MeV) - Penelope
214Bi β⁻ (max=3.3 MeV) - Geant4
210Tl β⁻ (max=4.4 MeV) - Penelope
210Tl β⁻ (max=4.4 MeV) - Geant4
214Bi (with 1-mm-Cu around ampoule)
210Tl (with 1-mm-Cu around ampoule)
Mean energy deposited in IC-gas region (eV)
6000
5000
4000
3000
600
300
0
1.3
1.4
1.5
1.6
1.7
1.8
1.9
gas-ampoule thickness (mm)

Fig. 5

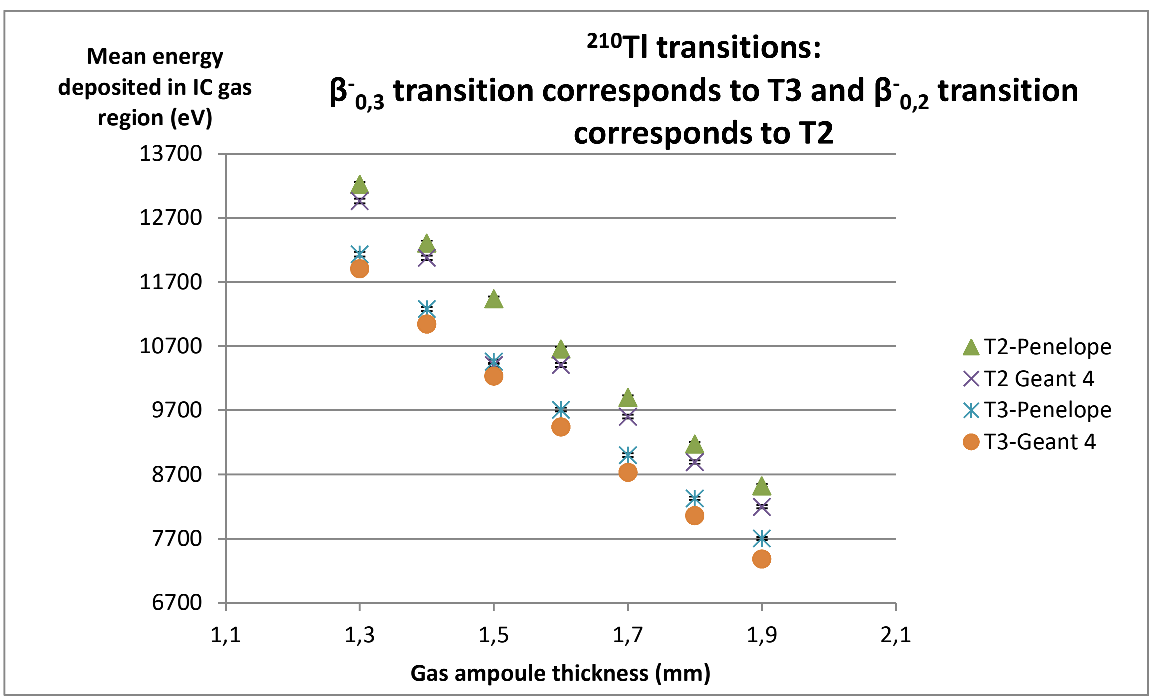
Mean energy deposited in IC gas region (eV)
210Tl transitions:
β-0,3 transition corresponds to T3 and β-0,2 transition corresponds to T2
13700
12700
11700
10700
9700
8700
7700
6700
1,1
1,3
1,5
1,7
1,9
2,1
Gas ampoule thickness (mm)
T2-Penelope
T2 Geant 4
T3-Penelope
T3-Geant 4

Fig.6:

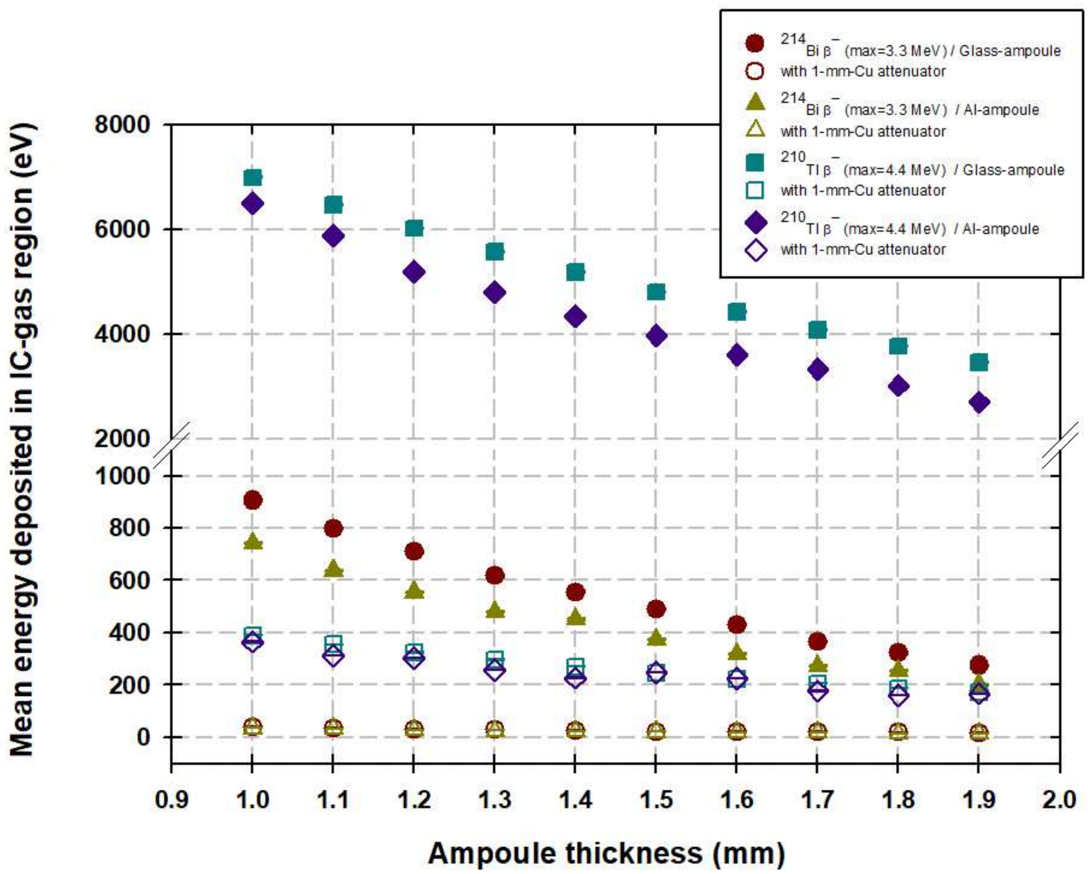

214Bi β− (max=3.3 MeV) / Glass-ampoule
with 1-mm-Cu attenuator
214Bi β− (max=3.3 MeV) / Al-ampoule
with 1-mm-Cu attenuator
210Tl β− (max=4.4 MeV) / Glass-ampoule
with 1-mm-Cu attenuator
210Tl β− (max=4.4 MeV) / Al-ampoule
with 1-mm-Cu attenuator
Mean energy deposited in IC-gas region (eV)
8000
6000
4000
2000
1000
800
600
400
200
0
0.9
1.0
1.1
1.2
1.3
1.4
1.5
1.6
1.7
1.8
1.9
2.0
Ampoule thickness (mm)

Table 1

Radionuclide	Daughter/^{222}Rn	Mode of decay	Energy (keV)	Intensity (%)
^{218}Po	1.00E00	$\beta^-_{0,0}$	260(12)	2.2 (3)
^{214}Pb	1.00E+00	$\beta^-_{0,0}$	1019 (11)	9.2 (7)
		$\beta^-_{0,4}$	724 (11)	41.09 (39)
		$\beta^-_{0,3}$	667 (11)	46.52 (37)
		$\beta^-_{0,7}$	485 (11)	1.047 (17)
		$\beta^-_{0,9}$	180 (11)	2.762 (22)
		$\gamma_{5,0}$	351.932 (2)	35.60 (7)
		$\gamma_{4,0}$	295.224 (2)	18.414 (36)
		$\gamma_{4,1}$	241.997 (3)	7.268 (22)
^{214}Bi	1.00E+00	$\beta^-_{0,28}$	822 (11)	2.76 (6)
		$\beta^-_{0,21}$	1066 (11)	5.642 (43)
		$\beta^-_{0,18}$	1151 (11)	4.339 (18)
		$\beta^-_{0,16}$	1253 (11)	2.449 (10)
		$\beta^-_{0,12}$	1423 (11)	8.147 (28)
		$\beta^-_{0,11}$	1506 (11)	17.494 (36)
		$\beta^-_{0,6}$	1727 (11)	3.12 (4)
		$\beta^-_{0,4}$	1892 (11)	7.45 (5)
		$\beta^-_{0,0}$	3270 (11)	19.67 (20)
		$\gamma_{1,0}$	609.312 (7)	45.49 (19)
		$\gamma_{4,1}$	768.356 (10)	4.892 (16)
		$\gamma_{6,1}$	934.061 (12)	3.10 (1)
		$\gamma_{9,1}$	1120.287 (10)	14.91 (3)
		$\gamma_{12,1}$	1238.111 (12)	5.831 (14)
		$\gamma_{4,0}$	1377.669 (12)	3.968 (11)
		$\gamma_{11,0}$	1764.494 (14)	15.31 (5)
		$\gamma_{21,0}$	2260.3 (2)	4.913 (23)
^{210}Pb	4.66E-04	$\beta^-_{0,1}$	17.0 (5)	80.2 (13)
		$\beta^-_{0,0}$	63.5 (5)	19.8 (13)
^{210}Bi	1.14E-04	$\beta^-_{0,0}$	1162.1 (8)	99.99986 (2)
^{210}Po	7.87E-7	$\alpha_{0,0}$	5304.33 (7)	99.99876 (4)

^{210}Tl	2.12E-04	$\beta^-_{0,11}$	1380 (12)	2
		$\beta^-_{0,10}$	1603 (12)	7
		$\beta^-_{0,9}$	1860 (12)	24
		$\beta^-_{0,8}$	2024 (12)	10
		$\beta^-_{0,7}$	2413(12)	10
		$\beta^-_{0,3}$	4290 (12)	31
		$\beta^-_{0,2}$	4386 (12)	13
^{206}Hg	8.85E-12	$\beta^-_{0,0}$	1308 (20)	62 (7)
^{206}Tl	1.68E-10	$\beta^-_{0,0}$	1532.4 (6)	99.885 (14)

Highlights:

- Simulation of the LNHB Vinten ionization chamber for ^{214}Bi and ^{210}Tl beta transitions.
- High-energy electrons from beta transitions can directly interact with the IC counting gas.
- IC response very sensitive to the ^{222}Rn ampoules wall thickness.
- This phenomenon may explain 5% discrepancies observed in the ^{222}Rn SIR comparison.